DESDE 2013
https://repository.uaeh.edu.mx/revistas/index.php/icbi/issue/archive
Pädi Boletín Científico de Ciencias Básicas e Ingenierías del ICBI

ISSN: 2007-6363

Publicación Semestral Pädi Vol. 13 No. 25 (2025) 246-254

Mineralization of REE found in the rift Molango, Mexico
Mineralización de REE encontrada en el rift Molango, México

R. G. Salinas-Maldonado [a], E. Salinas-Rodríguez [a], J. Hernández-Ávila [a], F. R. Barrientos-Hernández [a], E. Cerecedo-Sáenz [a], A. García-Cerón [a,*]

[a] *Área Académica de Ciencias de la Tierra y Materiales, Universidad Autónoma del Estado de Hidalgo, 42184, Pachuca, Hidalgo, México.*

Abstract

Strategic elements, such as rare earth elements and precious metals, are now of great economic importance for the development of industries and technologies; therefore, it is vital to discover and valorize the corresponding ore deposits that contain these valuable elements. This paper describes the correlation of the Rift (Molango) with sedimentary ore deposits, according to the tectonic and stratigraphic evolution of the place where the deposits were formed over time, the indirect method of exploration was used, using the analysis of geological transgressions. The mineralization found in these deposits contains elements from the platinum group and some light rare earth elements, which correspond to two types of formations: stratiform-type hosted sediments and stock work channels from the Lower Jurassic.

Keywords: Rift, REE's, Mineralization of PGE´s, Sedimentary Ores.

Resumen

Los elementos estratégicos, como los elementos de tierras raras y los metales preciosos, son ahora de gran importancia económica para el desarrollo de industrias y tecnologías; por lo tanto, es vital descubrir y valorizar los yacimientos minerales correspondientes que contienen estos valiosos elementos. En este trabajo se describe la correlación del Rift (Molango) con los yacimientos minerales sedimentarios, según la evolución tectónica y estratigráfica del lugar donde se formaron los yacimientos a lo largo del tiempo, se utilizó el método indirecto de exploración, mediante el análisis de las transgresiones geológicas. La mineralización encontrada en estos yacimientos contiene elementos del grupo del platino y algunos elementos ligeros de tierras raras, que corresponden a dos tipos de formaciones: sedimentos alojados de tipo estratiforme y canales stockwork del Jurásico Inferior.

Keywords: Rift • REE's, Mineralización de EGP, Menas sedimentarias.

1. Introduction

At present, exploration works are under way to locate mineral deposits of economic interest. This is why the study of geological structures, their formation processes and their influence on the enrichment of strategic and precious elements and rare earth elements (REE) for the development of new and better technologies is of such importance for the world economy.

In the same way, there is a large amount of evidence that relates the mineralization of different deposits to the evolution of specific geological structures. For the case of Rare Earth Elements (REEs) (Al Ani, et al. 2018), including fifteen lanthanides, yttrium and scandium, they are found in more than 250 minerals (Park, Seo, Lee, & Hyeong, 2019), worldwide. REE are used in various high-tech applications in several sectors, such as electricity and electronics, automotive, renewable energy, medicine (Nimila, et al., 2020) and defense.

In this context, the supply of REE are strategic, given their scarcity, in addition to providing important geological information. On the other hand, the scope of this work contributes to the exploration of REE in Mexico in the near future.

Likewise, the innovation of this study is based on the use of marine transgressions of heterochronous ages to locate possible exploration zones through the application of an indirect exploration method.

However, the rare earth minerals such as monazite, can occur

*Autor para la correspondencia: ga337807@uaeh.edu.mx
Correo electrónico: sa380249@uaeh.edu.mx (Ramón Guillem Salinas-Maldonado), salinasr@uaeh.edu.mx (Eleazar Salinas-Rodrígez), herjuan@uaeh.edu.mx (Juan Hernández-Ávila), profe_3193@uaeh.edu.mx (Francisco Raúl Barrientos-Hernández), eduardoc@uaeh.edu.mx (Eduardo Cerecedo-Sáenz)
Historial del manuscrito: recibido el 29/04/2024, última versión-revisada recibida el 31/10/2024, aceptado el 05/05/2025, en línea (postprint) desde el 16/05/2025, publicado el 05/07/2025. **DOI:** https://doi.org/10.29057/icbi.v13i25.12915

in different types of deposits such as the following: carbonatite rocks, hydrothermal, metasomatic rocks, granitoids/greisens, alkaline rocks, alkaline arkosic rocks, hydrothermal ore, Olserum-Djupedal Alkaline rocks, Nechalacho Carbonatite, Bayan Obo, Pegmatite (Yang, et al., 2024).

Also, the critical metal contents of four types of seabed mineral resources, including a deep-sea sediment deposit, are evaluatedas potential rare earth element (REE) resources: polymetallic nodules, ferromanganese crusts, deep-sea sediments and seafloor massive sulfides (Yu, et al., 2024).

For example, the Pb-Zn mineralization in the Morange in Pakistan, which is associated with the Jurassic period, was emplaced during the formation of the mountain range (synergetic), as well as at a later stage (epigenetic). This mineralization is of the SEDEX type (waliArain, et al., 2021), with argillaceous limestone forming a stratiform re-placement and pyrites on sphalerite matrix with galena in black shale, as well as vein-type fissure fills, composed of Lower Jurassic carbonates and a sequence of marine siliciclastic rocks. In some cases, evidence of remobilization can be observed, helping to establish a synsedimentary character, where the grain size of the minerals is often considerably fine (Ishihara, Kanehira, Sasaki, Sato, & Shimazaki, 1974) (Eldridge, Barton, & Ohmoto, 1983). Moreover, in supergenic Zn non-sulfide deposits, Fe oxyhydroxides become concentrated mainly in residual zones (Gossan) (Santoro, Putzolu, Mondillo, Boni, & Herrington, 2020), which are formed in systems containing certain elements, such as Zn, Pb, Co, REE, Sc, Ga, Ge, V, among others. Similarly, Cu-U-V deposits in the Eureka mine (northern Spain) that were emplaced in the same tectonic framework, hosted in Triassic red bed sandstones (Castillo-Oliver, et al., 2020), show supergenic alterations with nickel and cobalt dispersion. Vanadium was fixed as vanadates, while bismuth was fixed as oxide and rare earth phosphates as monazite and xenotime. This is important because it is widely accepted that red bed sedimentary deposits and other stratiform sedimentary deposits occur in such environments (Jowett, 1989).

Meanwhile, an outcrop in Mongolia has been described as showing Nb-Ta mineralization (Dostal & Gerel, 2022), which is present in a bimodal sequence of per-alkaline felsic rocks. There, tectonic processes produced the mineralization of Zr, Nb, heavy rare earth elements, Y, U, Th and Ta; while the per-aluminous felsic rocks formed Li-F via the mineralization of Sn, W, Ta, Li, and Nd. In addition, the occurrence of per-alkaline granites is present in northeast Mongolia, where Nd-Ta is associated with REE and zircon mineralization.

In the same way, it has been reported that there are alternative ways to locate rare earth elements that are found in the sediments of the ocean floor, the continental platform, rivers, streams and lakes. Likewise, there are phosphorite deposits comprising industrial waste products, such as red sludge, phosphogypsum, coal fly ash, mining waste, acid mine drainage and electronic waste (Balaram, 2023).

According to the Rift, this is a large crack in the Earth's crust, that began as a small crack derived from movements in the tectonic plates. As the tectonic plates interacted with each other, mainly in subduction zones, they caused geodynamic movement within the crust. For this reason, over millions of years, various types of mineralization were formed during or after the entire process and due to the phenomena associated with the stresses generated during the formation of the Rift.

Therefore, within the tectonic frameworks of different Rifts around the world, some types of mineralization have been found. For example, in Tongkuangyu in northern China, a Paleoproterozoric Cu mineralization has been described due to two formations: the first are red-layered copper sulfides that formed during metamorphic regression and the second are vein-type sulfides derived from the remobilization of first-stage sulfides via the infiltration of external fluids, such as residual seawater and metamorphic fluids, at surface level (Liu, et al., 2019).

Similarly, the gold mineralization in the Haoyaoerhudong Grabo in northern China is related to a Rift-type extensional structure, with high gold content (148 g/ton) hosted in Proterozoic strata that were generated in a post-orogenic extensional environment. This same Grabo has calcalkaline characteristics and demonstrate evidence of the enrichment of large ion lithophilic elements (LILE), as well as light rare earth elements (Wang, et al., 2019).

On the other hand, one of the world's largest deposits of Fe-REE-Nd can be found in Bayan Obo in Mongolia, which lies in a Rift-type structure (Kui-Feng, Hong-Rui, Pirajno, & Liu, 2023). Similarly, it has been determined that the fluids that form this mineralization are similar to those found in deposits located in various other parts of the world that contain carbonatites and alkaline igneous rocks with adequate REE contents. Additionally, other elements with Fe oxides and Cu- Au-REE content in associated igneous rock found in the Bayan Obo deposit have different fluid sources. Likewise, outcrops with good gold and Fe content have been located in some Rift- type structures (Wang, et al., 2019) in hydrothermal magmatic systems.

In this manner, the occurrence of REEs associated with Rift-like structures has been evidenced around the world, such as the case of the Abu Tartur sedimentary phosphate deposit (Obaidala, Mahfouz, & Metwally, 2023) and other deposits in China, Brazil, Vietnam, Canada, Russia, Nabimia, South Africa, and India (Balaram, 2023).

According to the above, it is necessary to provide an adequate description of Rift structures since, in many cases, they are associated with the occurrence of strategic REE, PGE, gold, among others (Ogden, et al., 2023).

Locating Rift-type structures, is carried out based on the specific geodynamic (Jara, Ghiglione, Galliani, & Mpodozis, 2023) stratigraphic and geochemical context. For example, cases where the areas to be studied are highly prospective for red bed (Silitoe & Rodríguez, 2023), or Mississippi Valley (Walter, et al., 2023) or SEDEX (Lisboa, Filho, Monteiro, & Mansur, 2023) ore deposits, which have a broad strategic significance, according to their base metal contents. So far, this type of prospecting has not been carried out in Mexico, so it would be interesting to carry out pioneering studies, such as that presented here, since they could provide valuable data on the presence of strategic minerals (REE) and elements from the platinum group (PGE).

In this way, this work contributes to the innovative consolidation of the exploration of strategic mineral since it has made it possible to validate areas of possible exploitation on the continent and can also minimize direct exploration costs.

Finally, the results shown here are effective and profitable,

since the possible geodynamic environment was determined by taking into account the classification parameters of Rift-type structures, beginning with the field assessment of strategic correlations related to contemporary marine transgressions in the Rift with mineral in areas that are currently visible.

2. Materials and Methods

To carry out this work, the methodology used was in accordance with the indirect prospecting method, widely described in previous work (Cerecedo-Sáenz, et al., 2018). Based in this work, in the first place, the field work was carried out searching for the base of the transgressive stage, which was previously identified as a marine siliclastic sequence from the Lower Jurassic. In this way, the information obtained was correlated with other outcrops such as the one found in the San Cayetano Formation in Matahambres, Cuba (Pérez-Vázquez & Melgarejo i Draper, 1998).

Firstly, in order to properly identify the outcrop and carry out sampling, it was analyzed the marine transgressions, and particularly considering the formations that contained sedimentary geological deposits from Lower Jurassic (Okita, 1992), integrating geological, stratigraphic and structural studies. Thus, when locating the outcrop, samples were obtained by drilling in the disclosed area. The holes were drilled using a portable drilling rig (JKS, Winkei, GW-15) with an air-cooled engine, which was gas-powered in two cycles. The drill cores obtained were from depths of 9 m and 0.03175 m in diameter.

The obtained samples were ground in a mortar and later were homogenized and quartered to obtain single homogeneous samples to be characterized. The characterization carried out in this work was executed in order to obtain accurate data for the mineralogical phases present. For this, an analysis of the general phases was conducted via X-Ray diffraction (XRD), for which the samples were ground down to an average particle size of less than 78 μm and put in an Equinox 2000 X ray Diffractometer (INEL, Artenary, France, located at UAEH), which was operated with a $CoK\alpha_1$ radiation. Phase identification was based on the COD Inorganics 2015 databases in the Crystallography Open Database Math! Software, (v.1.10, Crystal Impact, Bonn, Germany).

Additionally, our characterization studies employed scanning electron microscopy (SEM) to identify the texture, granulometry, and morphology of the detected phases. In the same way, X-ray mapping and energy dispersive spectrometry (EDS) helped us to determine the punctual and semi-quantitative compositions of some of the previously identified phases, using a JEOL scanning electron microscope model JSM-IT300 (JEOL Ltd, Tokyo, Japan, located at UAEH) and an OXFORD X-ray detector (OXFORD Instruments, Oxford shire, UK) with an acceleration voltage of 30 kV. In order to obtain a representative analysis, powder samples were placed on the specimen stubs in uniform layers and punctual quantitative routines were executed over large scanning areas (about 4.5 mm^2).

For chemical analysis, an inductively coupled plasma spectrometry (ICP-MS) analysis was conducted at Actlabs (Activation Laboratories Ltd., Ontario Canada) to find the average total rock compositions of the mineralized phases, for the identification of the positive anomalies for light rare earth elements and minerals from the platinum group (PGE). The methodology used in this case was the following; samples were fused and then diluted and analyzed by a Perkin Elmer Sciex ELAN 9000 ICP-MS spectrometer (Located at Actlabs, Canada). Fused blank was run in triplicate and duplicates were run every 10 samples, then instrument was recalibrated every 44 samples.

Finally, to determine the Au and Pt contents in the concentrates of the minerals, a cupellation analysis was carried out in an oven EMISION brand, CL Series. Samples preparation was done using borax, PbO, bone ash, sodium carbonate as flux, as well as silver (99.99 purity); melting temperature was of 1000°C during 90 minutes. After process, slag separation was done, obtaining a button containing the values of Ag, Pt and Au. Then, the release of Au from button was executed in porcelain crucibles on a heating plate at 100-120 °C, adding 15 % nitric acid to dissolve Ag, obtaining a solution of silver nitrate. Then release of Au and Pt was done using aqua regia adding 10 % of hydrochloric acid with stirring in test tubes. The determination of Au and Pt contents was done using a ICP- OES Varian brand 735ES ICP (Located at the Pachuca and Real del Monte mining company, Mexico), where samples were analyzed with a minimum of 10 certified reference materials, all samples were prepared using sodium peroxide fusion. Every 10 samples were prepared in this way and analyzed by duplicate, and the blank was renewed every 30 samples. Internal standards were used as part of the standard operations procedure of equipment.

3. Results

3.1. Description of the formation of the rift and the associated mineralization

First, through the evaluation of all data obtained in the field work and with the help of the indirect method of exploration, the information necessary for determining the existence of the Rift was obtained. Figure 1 shows a model of the formation dynamics of said Rift, which is centered on geodynamic extension mechanisms. The heterochronic ages could be defined using the typical mineralization. The idealized model of the occurrence of an exhalative sedimentary reservoir (SEDEX) that on the flanks rests on tectonic pillars, is of Precambrian age. It starts with the expansion of the reducing basin with siliciclastic clasts from a Triassic-Jurassic transgression; followed by the oxygenation of the basin and a subsequent transgression during the Upper Jurassic, and finally Tertiary volcanism that crowns the sequence.

According to the analysis, the transgressive geological formation was identified as Huayacocotla Formation of Lower Jurassic (Pleisnbachian) with a thickness of 600 m, which is of mining interest. Its upper contact was from the Middle Jurassic Tepexic Formation, while the lower contact rested in angular unconformity on a Paleozoic and Precambrian sequence.

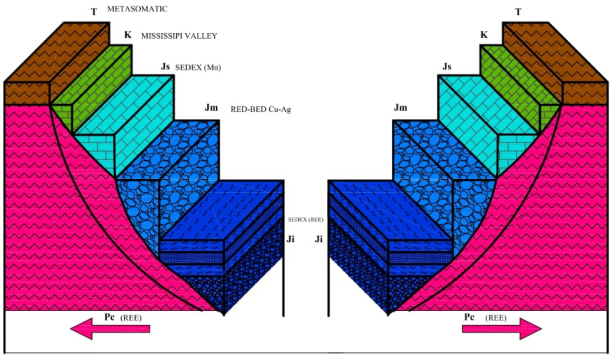

Figure 1: Model representing the formation of SEDEX within a rift structure and its mineralization.

It was identified that the mineralization was due to an extension event, that occurred during the lower Jurassic period, which concluded in the Middle Jurassic and formed horsts and grabens of NW-SE and N-S faults. All the faults bordered a crystalline basement. This period was associated with the origins of the Gulf of Mexico during the opening of Pangea. On the other hand, there was also evidence of the abrupt lateral termination of the middle Jurassic Cahuasas Formation, the occurrence of what is interpreted as graben deposits in bands and was a consequence of Rift evolution.

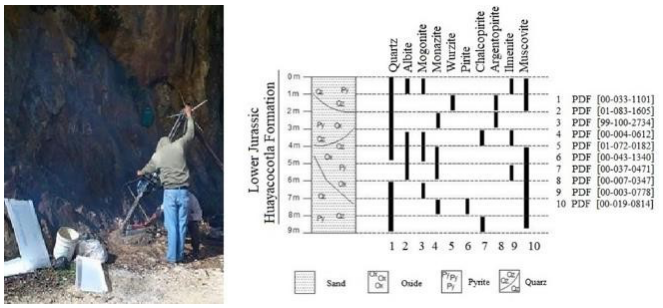

Figure 2: Drilling stage, XOCH 1. Right shows the drilling process and the left shows the mineral phases obtained from the drilling cores (by XRD).

Likewise, in the study area, two important tectonic events were additionally identified. However, they were not directly related to the mineralization studied. The first was a continued subsidence and marine transgression, which demonstrated a lithological change from a siliciclastic sequence to a normal marine carbonate deposit during the Upper Jurassic, as with the Santiago, Chipoco and Pimienta Formations. These conditions persisted into the late Cretaceous, in addition to folds during the Late Cretaceous Eocene, as with the Laramide Orogeny. The second event was a post-Pliocen extension with the presence of normal faults.

Consequently, perforation was carried out (XOCH 1 well, Figure 2) using the mineralization data. During the drilling of this lithological unit, lateral changes in the size of the clasts were observed, as well as a change in the rate of sedimentation.

Based on the detailed analysis of the drilling cores and the correlations between the outcrops, it was possible to see that the formation consisted of three members. At the base, it had conglomerates, sandstone and shale, which contained exoclasts with fusilinids and was characterized by the absence of autochthonous fossils.

At the base of this outcrop, there was possibly a small interval of the oldest limestone unit that, in its complete sequence included conglomerate, sandstone, siltstone, and shale with gap intervals, reworked fossils, sandstone exoclasts, volcanic rock fragments and a small proportion of limestone. The size of the measured clasts was from 5 to 100 cm in a sandy matrix and the size of the clasts in the conglomerate, suggested a continental affinity.

The middle member was made up of conglomerates, sandstone and shale, and was characterized by the presence of ammonites. Finally, in the upper portion there was sandstone, siltstone and shale, with very few conglomerates, which ranged in thickness from 0-1 to 600 m. There were veins of stock work that were contemporaneous with mineralization. Likewise, the mineralization in the sedimentary lithology was enriched with precious metals. In the production unit and the unit that overly it, sandstone lenses were observed, along with some rich organic matter that framed a reducing environment.

For the SEDEX base metal deposits, these were only located in the intermediate unit of transgressive lithology, comprising shale and sandstone in rhythmic intervals, which overlaid the shale unit with plants from the Huayacocotla Formation. The greatest presence of monazite was observed in the unit with shale and a high carbon content, at the base of the intermediate unit, where the exhalative roots appeared.

The intermediate unit represented a marine transgression because it consisted of sandstone and shale in a rhythmic sequence. The main characteristic of this unit was the presence of marine ammonites at its base, mainly in the shale. Additionally, the exhalative roots of the outcrop were observed near to the top.

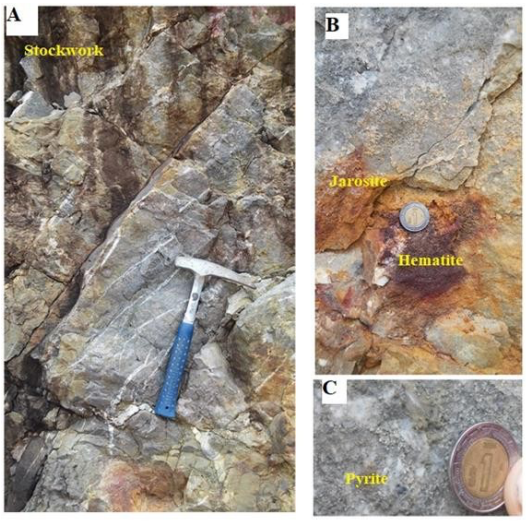

Figure 3: Mineralization zone. Showing the stckwork (A), the presence of Fe like jarosite and hematite (B), and pyrite (C)

According to the results, there was only one possible producer mining horizon located in the middle part of the study area, close to the top of the Pleinsbachian Huayacocotla Formation from the Lower Jurassic period. However, some exhalative roots could be seen in the initial portion of the transgressive cycle. Figure 3 shows the mineralization of the exhalation roots of a stock work type (Figure 3A), jarosite and hematite (Figure 3B), and disseminated pyrite (Figure 3C).

It is worth mentioning that, in this area, there was an inverse fault (Figure 4A) in contact with the mineralization (Figure 4B) because the intermediate member that contained ammonites was in contact with the organic carbon upper member (Figure 4C), was made of sandstone, siltstone, slate, some conglomerates, and fossilized plants. In this last member near the top of the Huayacocotla Formation, the potential producer mining horizon was found.

In the study area, the producer unit was 900 m from the Huayacocotla Formation and was 350 m thick. The thickness of the producer horizon surfaced at 100 m. The upper shale unit comprised sedimentary rocks with plants was 250 m high increasing to 350 m high in some areas with volcanic rock outcrops. The intermediate member was more than 250 m thick and the base member was about 450 m thick.

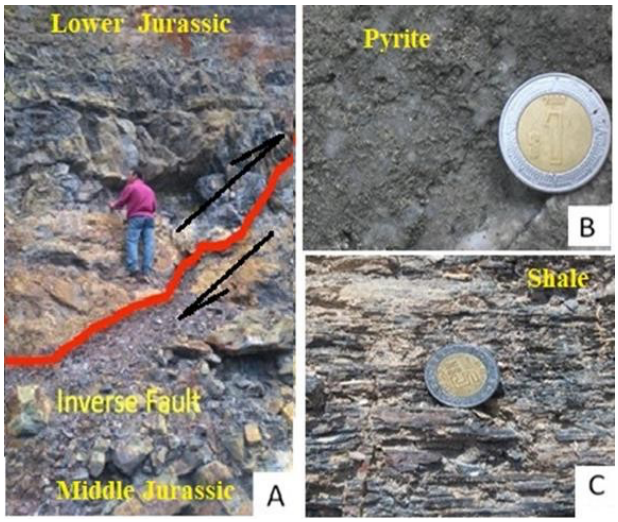

Figure 4: Huayacocotla Formation. Showing the inverse fault (A), disseminate pyrite (B) and shale (C).

The geological mining behavior was different at the Huayacocotla Formation, since the SEDEX mineralization was only attributed to the lithology of the intermediate member, comprising shale and plants. In Figure 5, the hydrothermal system hosting the epithermal veins was characterized by a length of 15 km, heat flux and mass flux of fluid that were steady relative to the timescale of the vein formation. The figure shows the localization of the veins near the faults in the system. The hydrothermal system containing the veins applied bark-style surfaces to a wide range of deposits in the process of heat extraction, which is associated with fragile deformation. The deposits included epithermal veins, massive seafloor sulfides, mesothermal veins in cortical zones, high-temperature veins and hypothermic stock work.

On the other hand, Ag and Au base metals and epithermals are developed in many hundreds of meters from the surface of the hydrothermal system; such as chalcopyrite followed by strong hydrothermal activity of albite and muscovite, reaching high temperatures, as moganite and iron oxides with some REE contents.

In the same way, rock alterations were observed and in the field work were profusely found vein systems developed in hydrothermal systems that were related to relative faults with approximately NNW SSE direction, whose tectonic persisted by a possible reactivation in the Pliocene.

In Figure 5, the orientation, scale range and spatial frequency of the veins is related to the nature of the host rock depending on whether it is lode or sedimentary.

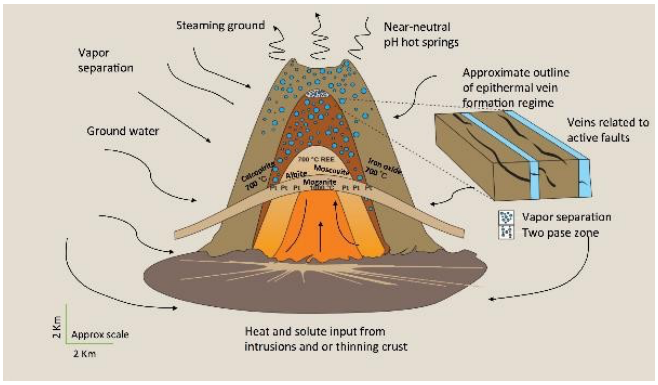

Figure 5: Description of the model for the Hydrotermal system and veins.

3.2. Characterization of SEDEX ore body

3.2.1. X- ray Diffraction

The results of the X-ray diffraction (XRD), showed in Figure 6, confirm the presence of high- and medium-temperature minerals, such as quartz, monazite, and ilmenite. Interestingly, the presence of ilmenite could be associated with rare earth elements.

The minerals shown in Figure 6 were evidence of hydrothermal remobilization, confirming that the deposit found was of the SEDEX type.

It can also be seen that there were high- and medium-temperature minerals distributed throughout the lithological column, confirming the existence of thermal pulses.

Also, Quartz was distributed throughout the column from 1 to 4.75 m, and from 6 to 9 m, except from 4.75 to 6 m, which indicated the existence of alpha quartz that was formed at a temperature of 870 °C and was also found in the form of moganite at 1, 4 and 5 m depth and that was formed a high temperature of 1627 °C. Albite was found from 1 to 1.75 m, and from 4 to 6.75 m, but was abscent at 2, 3, 7, 8 and 9 m, to the center of the column.

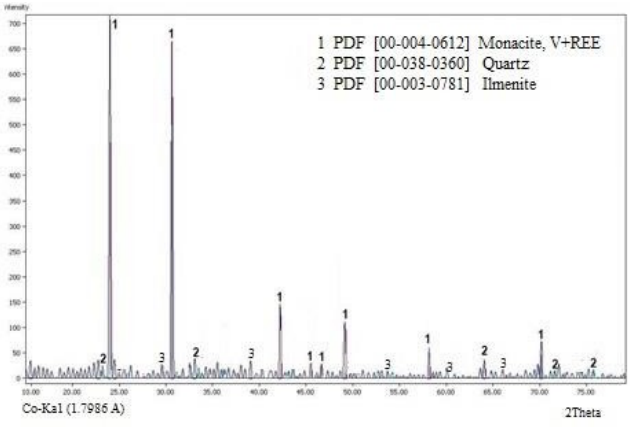

Figure 6: X-Ray Diffraction spectra of SEDEX mineral emplaced during the formation of the Rift.

3.2.2. Scanning Electron Microscopy (EDS & X-ray Mapping)

Figure 7 shows micrographs of the original minerals, taken from the core drills at a depth of 100 cm, which had high silicification and very disseminated pyrite in the matrix. Sinuous surfaces could be observed, comprising particles that were from 6.6 to 21 μm in size and had euhedral structures.

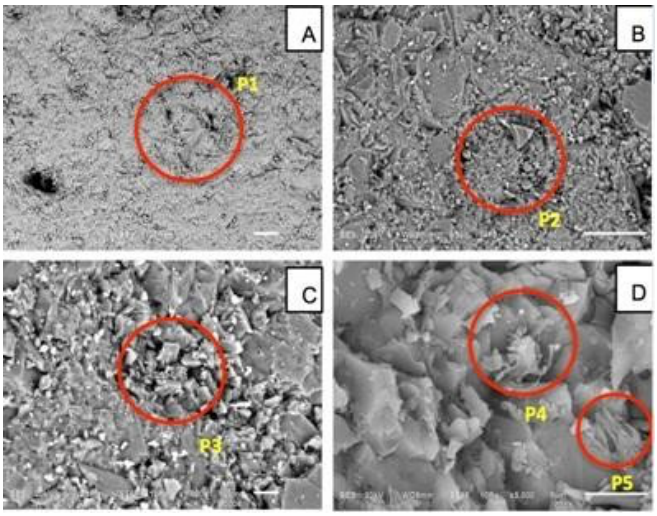

Figure 7: SEM images of the particles of SEDEX-type mineral.

The images show the similar microstructures, along with the variations in their shapes (euhedral, anhedral and subhedral) and surfaces (smooth, fibrous and sinuous). Additionally, it can be seen that there was a wide distribution of sizes no greater than millimeters. Figure 7A shows an aphicitic structure in central area P1, indicating the location of a tubular crystal (greater than 100 m) that was potentially quartz. Figure 7B also shows twinned prismatic crystals (P2) with an average size of 25 μm, which were potentially albite.

Additionally, Figure 7C shows (P3) twinned albite crystals and more small cubic crystals of pyrite or marcasite, which were no longer than 10 μm. Finally, Figure 7D shows alteration minerals, which had fibrous textures (similar to those of clay and cubic crystals) (P4 and P5), and were 1 μm size.

According to the above, along with the results of the ICP (total rock), it was able to confirm the presence of these strategic elements in the SEDEX-type deposit, which formed the basis of the potential for this deposit to be economically attractive. According to the values obtained by ICP analysis, Table 1 shows the chemical compositions of the two samples obtained form the core drill.

Table 1: Chemical composition obtained by ICP, in μg/g.

Element	Sample 1	Sample 2
Au	0.02	0.02
Pd	0.05	0.05
Pt	0.05	0.05
Al	9000	8100
As	28	119
B	70	70
Ba	82	67
Be	3	3
Bi	2	2
Ca	1700	13
Cd	2	2
Ce	19.5	14.9
Cr	30	30
Cs	2.3	2.7
Cu	7	7
Dy	1.5	1.4
Er	0.9	0.9
Eu	0.4	0.3
Fe	9200	1640
Ga	2.5	2.2
Gd	1.6	1.4
Ge	1.3	1.5
Hf	10	10
Ho	0.3	0.3
In	0.02	0.02
K	2000	2000
La	9	7
Li	49	71
Mg	800	500
Mn	85	104
Mo	2	1
Nb	2.4	1
Nd	9.5	7.6
Ni	10	10
P	50	50
Pb	11.1	7.5
Pr	2.5	1.9
Rb	17.1	15.8
S	7500	1460
Sb	2	2
Sm	1.9	1.6
Sn	0.7	0.5
Sr	8	9
Tl	10.1	5.8
Tb	0.3	0.2
Te	6	6
Th	1.8	1.4
Ti	800	700
Ta	0.6	0.4
Tm	0.1	0.1
U	1.3	1

V	17	28
W	0.7	0.7
Y	8.8	7.7
Yb	0.7	0.7
Zn	30	30
Si	39400	40800

Finally, Table 2 shows the average element distribution in the samples, pointint special attention to the principal elements such as rare earth elements, Au, Pd and Pt, among others. Where the contents are shown in major, minor, and trace elements, and can be confirmed the presence of rare earth elements.

Table 2. Average chemical composition obtained from the table 1

Element	Units	Concentration
Ce, Nd, La, Eu, Gd, Sm, Y	µg/g	0.4-19.5
Au, Pd, Pt	µg/g	0.02-0.05
Ti, Si, Mg, Fe, Al, K	µg/g	800-40800

4. Discussion

There are two controversial aspects in this work, the classification of the deposit and the mineral association. In the first case, it was considered to be SEDEX-type mineralization because two types of mineralization were recognized: filonian and strati-form like was reported before (Pérez-Vázquez & Melgarejo i Draper, 1998). In the filonian exhalation, roots were observed in the stock work towards the base, which did not of course cut the top of the sedimentary sequence. Here, it is inferred that they can correspond to the emission channels, as was pointed by Wang et al (Wang, et al., 2023).

Meanwhile, the mineralization SEDEX type (Jowett, 1989) is stratiform and concordant with shales, slate sediments of submarine origin, which is the same as that in some zones, showing great schistosity (Cawood, Rozendaal, & Spyr, 2023) and faults (Creus, Sanislav, Dirks, Jago, & Davis, 2023). The reason why it could be inferred that the age of this mineralization is before to the development of the mountains and hills in this area, is because their association with schistosity and pyrite. Additionally, it was inferred here that, perhaps due to reductive conditions, the precipitation of the sulfides observed in the hand specimen was favored, such as the finely disseminated pyrite (Okita, 1992) and sphaletite in minor proportion (Liu, et al., 2023), which in some cases, shows framboidal crystallization (Conde, Tornos, Danyushevsky, & Large, 2021) and botroydal growths, proposing that its formation corresponds to a chemical nature, formed in a submarine media (Ishihara, Kanehira, Sasaki, Sato, & Shimazaki , 1974) (Eldridge, Barton , & Ohmoto, 1983). So, all this approaches to a SEDEX mineralization of the Selwyn type (Williams), because the nature of the Huayacocotla Formation of the Lower Jurassic Age is of the siliciclastic type of a reducing environment of the SEDEX- type ore (waliArain, et al., 2021) (Ogden, et al., 2023). Finally, the above was due to the low amount of nickel and other metallic contents such as chromium and the association of Fe and Mg (Staude, Raisch, & Markl, 2023). Similarly, other elements of ultra-basic affinity were present in this mineralization, and the additional results found allow this site to be classified as SEDEX (Obaidala, Mahfouz, & Metwally, 2023) (Ogden, et al., 2023). However, considering these results and the important contents of platinum in metallic form, this deposit can be sub-classified as a more regional subtype.

5. Conclusions

1. According to the indirect exploration method used, this indicated that the Huayacocotla Formation is favorable for exploration of SEDEX deposits, in a deeper way.
2. The outcrops could be observed with the abrupt lateral termination of the Cahuasas Formation and its distribution in parallel bands, was as a consequence of the rupture of the Rift in the region.
3. High silicification was observed with zones of disseminated pyrite found in normal faults between Precambrian Gneiss and Paleozoic volcano-sedimentary rocks, which were active when the Huayacocotla Formation was deposited.
4. The mineralogy of the outcrop showed a clear and continuous mineralogical zoning that is reflected by the contents of Au, Pt, V, Cr, Cu, Ag, Zn, Pb and Ba.
5. The high-temperature exhalative minerals found, were ilmenite, monazite, and moganite.
6. The medium- temperature minerals that mark the end of the pulse, were albite type (NaAlSi3O8), and chalcopyrite as the typical mineral of hydrothermal solutions remobilization.
7. Anomalies of V and Cr (determined by ICP-MS) were also observed, which could be associated with the metal contents of the platinum group.
8. The characterization done through ICP-MS allowed determining the presence of REE and PGE, the latter not previously known in Mexico. Like Ce, Nd, La, Eu, Gd, Sm, and Y (ranging from 0.4 to 19.5 µg/g); and Au, Pd and Pt (ranging from 0.02 to 0.05 µg/g).
9. Finally, the results found in this work could be used to find ore deposit near to the exploration are, with contents of REE and PGE higher that could be exploited.

Acknowledgments

Authors want to thanks to UAEH, for the facilities given during the elaboration of this work.

References

Al-Ani, T., Molnár, F., Lintinen, P., & Seppo, L. (2018). Geology and Mineralogy of Rare Earth Elements Deposits and Occurrences in Finland. *Minerals, 8*(8), 356. doi:https://doi.org/10.3390/min8080356

Balaram, V. (2023). Potential Future Alternative Resources for Rare Earth Elements: Opportunities and Challenges. *Minerals, 13*(3), 425. doi:10.3390/min13030425

Castillo-Oliver, M., Melgarejo, J., Torró, L., Villanova-de-Benavent, C., Campeny, M., Díaz-Acha, Y., Tualer, E. (2020). Sandstone-Hosted Uranium Deposits as a Possible Source for Critical Elements: The Eureka Mine Case, Castell-Estaó, Catalonia. *Minerals, 10*(1), 34. doi:https://doi.org/10.3390/min10010034

Cawood, T., Rozendaal, A., & Spyr, P. (2023). Discussion on "Syn-metamorphic sulfidation of the Gamsberg zinc deposit, South Africa" by Stefan Höhn, Hartwig E. Frimmel, and Westley Price. *Mineralogy and Petrology, 117*, 775-785. doi:https://doi.org/10.1007/s00710-023-00821-6

Cerecedo-Sáenz, E., Rodríguez-Lugo, V., Hernández-Ávila, J., Mendoza-Anaya, D., Reyes-Valderrama, M., Moreno-Pérez, E., & Salinas-Rodríguez, E. (2018). Mineralization of Rare Earths, Platinum and Gold in a Sedimentary Deposit, Found Using an Indirect Method of Exploration. *Aspects in Mining & Mineral, 1*(2). doi:10.31031/AMMS.2018.01.000510

Conde, C., Tornos, F., Danyushevsky, L., & Large, R. (2021). Laser ablation-ICPMS analysis of trace elements in pyrite from the Tharsis massive sulphide deposit, Iberian Pyrite Belt (Spain). *Journal of Iberian Geology, 47*, 429-440. doi:10.1007/s41513-020-00161-w

Creus, P., Sanislav, I., Dirks, P., Jago, C., & Davis, B. (2023). The Dugald River-type, shear zone hosted, Zn-Pb-Ag mineralisation, Mount Isa Inlier, Australia. *Ore Geology Reviews, 155*. doi:https://doi.org/10.1016/j.oregeorev.2023.105369

Dostal, J., & Gerel, O. (2022). Occurrence of Niobium and Tantalum Mineralization in Mongolia. *Minerals, 12*(12). doi:https://doi.org/10.3390/min12121529

Eldridge, C., Barton , P., & Ohmoto, H. (1983). Mineral Textures and their Bearing on Formation of The Kuroko Orebodies. *Economic Geology Monograph, The Kuroko and Related Volcanogenic Massive Sulfide Deposits, 5*, 241-281. doi:10.5382/Mono.05.15

Ishihara, S., Kanehira, K., Sasaki , A., Sato, T., & Shimazaki , Y. (1974) Geology of Kuroko deposits. *Minerals, 6*, 435.

Jara, R., Ghiglione, M., Galliani , L., & Mpodozis, C. (2023). From rift to foreland basin: A case example from the Magallanes-Austral basin, southernmostAndes. *35*, 865 - 897. doi:https://doi.org/10.1111/bre.v35.3

Jowett, E. (1989). Effects of Continental Rifting on the Location and Genesis of Stratiform Copper-Silver Deposits. Sediment-hosted stratiform copper deposits. *Geological Association of Canada, 36*, 53-66.

Kui-Feng, Y., Hong-Rui, F., Pirajno, F., & Liu, X. (2023). . Magnesium isotope fractionation in differentiation of mafic-alkaline-carbonatitic magma and Fe-P-REE-rich melt at Bayan Obo, China. *Ore Geology Review, 157*. doi:10.1016/j.oregeorev.2023.105466

Lisboa, L., Filho, C., Monteiro, L., & Mansur, E. (2023). Gahnite, garnet and magnetite compositions of metamorphosed sediment-hosted Zn- Pb-(Cusingle bondAg) deposits of the Mesoproterozoic Nova Brasilândia Group: Vectors for SEDEX deposits with Broken Hill- type affinities in the western Amazonian Craton, Brazi. *Journal of Geochemical Exploration, 249*. doi:https://doi.org/10.1016/j.gexplo.2023.107210

Liu, W., Mei, Y., Etschmann, B., Glenn, M., MacRae, C., Spinks, S., . . . Paterson, D. (2023). Germanium speciation in experimental and natural sphalerite: Implications for critical metal enrichment in hydrothermal Zn-Pb ores. *Geochimica et Cosmochimica Acta, 342*, 198-214. doi:https://doi.org/10.1016/j.gca.2022.11.031

Liu, X., Yang, K., Rusk, B., Oui, Z., Hu, F., & Pironon, J. (2019). Copper Sulfide Remobilization and Mineralization during Paleoprotezoric Retrograde Metamorphism in the Tongkuangyu Copper Deposits, North China Craton. *Minerals, 9*(7), 443. doi:10.3390/min9070443

Nimila, D., Nadeera, B., I.M.S.K, I., Sudath, R., Ranjith, P., Bandara, A., . . . Kithsiri, D. (2020). The story of rare earth elements (REEs): Occurrences, global distribution, genesis, geology, mineralogy and global production. *Ore Geology Reviews, 122*. doi:https://doi.org/10.1016/j.oregeorev.2020.103521.

Obaidala, N. A., Mahfouz, K. H., & Metwally, A. A. (2023). Mesozoic Sedimentary Succession in Egypt. . In *The Phanerozoic Geology and Natural Resources of Egypt* (pp. 169-219). Springer International Publishing. doi:https://doi.org/10.1007/978-3-030-95637-0_6

Ogden, C. S., Bastow, I. D., Ebinger, C., Ayele, A., Kounoudis, R., Musila, M., Kibert, B. (2023). The development of multiple phases of superposed rifting in the Turkana Depression, East Africa: Evidence from receiver functions. In *Earth and Planetary Science Letters* (Vol. 609). doi:10.1016/j.epsl.2023.118088

Okita, P. (1992). Manganese carbonate mineralization in the Molango District, Mexico. *Economic Geology, 87*(5), 1345-1366. doi:https://doi.org/10.2113/gsecongeo.87.5.1345

Park, S. J., Seo, I., Lee, K. Y., & Hyeong, K. (2019). Rare Earth Elements and Other Critical Metals in Deep Seabed Mineral Deposits: Composition and Implications for Resource Potential. *Minerals, 9*(3). doi:https://doi.org/10.3390/min9010003

Pérez-Vázquez, R., & Melgarejo i Draper, J. (1998). El yacimiento Matahambres (Pinar del Río, Cuba): estructura y mineralogía (in Spanish). *Acta geológica hispánica, 33*(1), 133-152. Retrieved from https://raco.cat/index.php/ActaGeologica/article/view/75549

Santoro, L., Putzolu, F., Mondillo , N., Boni, M., & Herrington, R. (2020). Influence of Genetic Processes on Geochemistry of Fe-oxy-hydroxides in Supergene Zn Non-Sulfide Deposits. *Minerals, 10*(7), 602. doi: https://doi.org/10.3390/min10070602

Silitoe, R., & Rodríguez, G. (2023). Exhalative red-bed copper mineralization in travertine, Puna Plateau, northwest Argentina. *Mineralium Deposita, 50*, 243-261. doi:https://doi.org/10.1007/s00126-022- 01134-y

Staude, S., Raisch, D., & Markl, G. (2023). Sulfide anatexis during high-grade metamorphism: a case study from the Bodenmais SEDEX deposit, Germany. *Mineralium Deposita, 58*, 987-1003. doi:https://doi.org/10.1007/s00126-023-01166-y

waliArain, A., ShakoorMastoi, A., DaaharHakro, A., AhmedRajper, R., AfzalJamali, M., & RazaBahatti, W. (2021). A preliminary review on the metallogeny of sediment-hosted Pb-Zn deposits in Balochistan, Pakistan. Earth Science Malaysia (ESMY), 5, 19-26. doi:10.26480/esmy.01.2021.19.26

Walter, B., Giebel, R., Siegfried, P., Doggart, S., Macey, P., Schiebel, D., & Kolb, J. (2023). The genesis of hydrothermal veins in the Aukam valley SW- A far field consequence of Pangean rifting? Journal of Geochemical Exploration, 250. doi:https://doi.org/10.1016/j.gexplo.2023.107229

Wang , J., Wang, X., Liu , J., Liu, Z., Zhai, D., & Wang, Y. (2019). Geology, Geochemistry, and Geochronology of Gabbro from the Haoyaoerhudong Gold Deposit, Northern Margin of the North China Craton. Minerals, 9(1), 63. doi:10.3390/min9010063

Wang, J., Xuexiang, G., Jinchi, X., Yongmei, Z., Yiwei, P., & Liangtao, L. (2023). New Insights into the Tectonic Setting and Origin of the Haerdaban Pb-Zn Deposit. Chinese Western Tianshan: Evidence from Geological, Chert Geochemistry, and Detrital Zircon U-Pb Geochronology. 57. doi:https://dx.doi.org/10.2139/ssrn.4477187

Williams, N. (n.d.). Light-Elements Stable Isotope Studies of the Clastic-Dominated Lead-Zinc Mineral Systems of Northern Australia and the North American Cordillera: Implications for Ore Genesis and Exploration. Isotopes in Economic Geology, Metallogenesis and Exploration, 2023, 329-372. doi:https://doi.org/10.1007/978-3- 031-27897-6_11

Yang, Y., Song, W., Liu, Y., Zhu, X., Kynicky , J., & Chen, Q. (2024). Mineralogy and element geochemistry of the Bayan Obo (China) carbonatite dykes: Implications for REE mineralization. Ore Geology Reviews, 165, 15. doi:https://doi.org/10.1016/j.oregeorev.2024.105873

Yu, L., Zou, H., Li, M., Pirajno, F., Cao, H., Xiao, B., Hou, M. (2024). Fingerprinting Pb-Zn mineralization events in the SW Yangtze Block, South China: A case from Yuanbaoshan deposit. Ore Geology Reviews, 165. doi:https://doi.org/10.1016/j.oregeorev.2024.105878.